COLOR IMAGES WITH THE MIT HOLOGRAPHIC VIDEO DISPLAY

Pierre St-Hilaire, Stephen A. Benton, Mark Lucente, Paul M. Hubel
Spatial Imaging Group
MIT Media Laboratory
Cambridge, MA

ABSTRACT

The MIT holographic video display can be converted to color by illuminating the 3 acoustic channels of the acousto-optic modulator (AOM) with laser light corresponding to the red, green, and blue parts of the visible spectrum. The wavelengths selected are 633 nm (red), 532 nm (green), and 442 nm (blue).

Since the AOM is operated in the Bragg regime, each wavelength is diffracted over a different angular range, resulting in a final image in which the three color primaries do not overlap. This situation can be corrected by shifting the diffracted spatial frequencies with an holographic optical element (HOE). This HOE consisting of a single grating is placed right after the AOM in the optical setup. Calculation of the required spatial frequency for the HOE must take into account the optical activity of the TeO_2 crystal used in the AOM. The HOE introduces distortions in the final image, but these are so small as to be visually negligible. The final images are of a good quality and exhibit excellent color registration. The horizontal view zone, however, diminishes for the shorter wavelengths.

I. INTRODUCTION

The MIT electronic holography display has demonstrated the possibility of displaying good quality computer generated holographic images of a reasonable size and resolution[1,2,3,4] . Visitors at our laboratory have frequently asked if such a technology could be converted to the display of color images. The present paper demonstrates that it is indeed possible to obtain color images exhibiting an excellent gamut and color rendition by the use of carefully selected laser wavelengths and a simple holographic optical element (HOE).

In this paper we will first describe how the optical activity of the tellurium dioxide (TeO_2) acousto-optic crystal affects the optical design of the color display. We then demonstrate a simple technique for color registration with an HOE. Finally we will describe the results of our experiments and point to possible ameliorations of our process.

II. DISPLAY TECHNOLOGY

The operation of the display has been described in various publications[1,2,3,4] and will be briefly summarized as follows:

The fundamental idea behind the MIT holo-video display is the use of an acousto-optic modulator (AOM) as the medium in which the holograms are written. The AOM consists of a single transparent TeO_2 crystal operated in the slow shear mode. At one end of the crystal is an ultrasonic transducer, which converts the electrical holographic information signal to an acoustic wave that is launched down the crystal. As the acoustic wave propagates, the regions of elastic shear present a modulated index of refraction to the optical beam, which passes perpendicularly to the acoustic wave. The optical beam thus emerges from the crystal with a relative phase-difference pattern across its width that is proportional to the instantaneous amplitude of the acoustic wave along the length of the crystal. This complex fringe pattern transfers the CGH data to

the optical beam. Its operating RF spectrum ranges from 50 to 100 MHz. Because its total angle of diffraction range is only 3 degrees, a demagnification factor is needed to bring the viewing angle to a more acceptable value (typically 15 degrees).

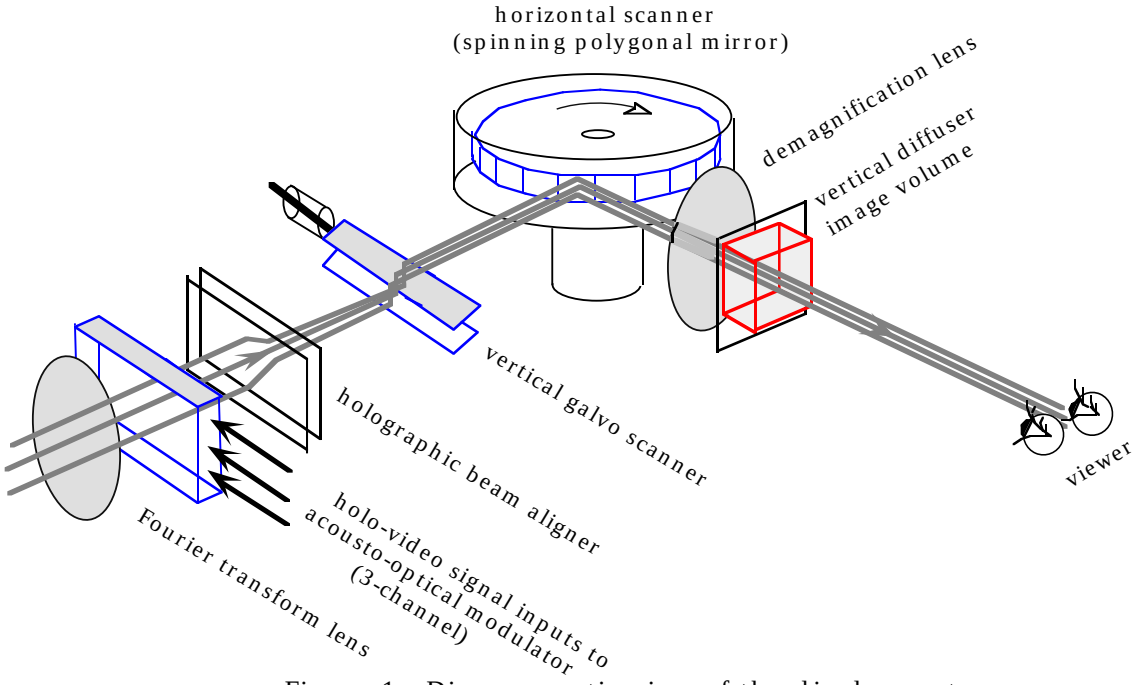

Figure 1. Diagrammatic view of the display system.

In the AOM, the fringes propagate at a rate of 617 meters/second, which is the speed of shear waves in the TeO_2 crystal. Therefore, the diffracted image also moves (from left to right) at this rapid rate. In order to make the image appear stationary, a spinning polygonal mirror is used to scan the image of the AOM in the opposite horizontal direction. The horizontal scan also acts to multiplex the image of the crystal, creating a virtual crystal that is exactly as long as one line of the CGH. This multiplexing is necessary because the crystal can hold only a small fraction of the total number of fringes at a time. The vertical deflection is provided by a closed loop galvanometric scanner.

It is possible to write independent diffraction patterns simultaneously on the crystal by using an array of transducers[5]. Under the right conditions such a technique can multiply the vertical resolution by a factor equal to the number of transducers without significant interchannel crosstalk. Such a technique has been demonstrated with a 3 channel AOM[4] and is depicted in Figure 1. In the case of the 3-channel AOM the holographic signal is provided by the red, green and blue outputs of a high bandwidth framebuffer which has been modified to suit our purposes. Using this technique we have achieved good images having a volume of a cubic inch, a horizontal viewing angle of 12 degrees, and a vertical resolution of 192 scan lines.

III. TRADING VERTICAL RESOLUTION FOR COLOR

It is possible to use each of the three independent channels of the AOM for the implementation of a color display at the expense of vertical resolution. For this purpose we need to illuminate each of the properly computed diffraction patterns on the crystal with red, green and blue laser light and adequately register the corresponding images. The vertical resolution will be reduced to a third of its previous value. Different issues need to be adressed for a successful completion of such an effort:

1 - Choice of proper primary wavelengths.
2 - Hologram computation.
3 - Vertical image registration.
4 - Horizontal image registration.

Those issues will be explored in the following sections.

IV. CHOICE OF PRIMARY WAVELENGTHS

Many studies have been published in the last few years concerning the proper rendition of color images in holography[6,7,8]. Using the right wavelengths for the red, green, and blue components of the image is essential to assure a good gamut. Moreover, the selected wavelengths should be easily available using commercial lasers. Recent work by Hubel has demonstrated this to be indeed possible[9]. In the course of our work we have investigated combinations of the following primary wavelengths:

Red primary: 633 nm (HeNe).
Green primary: 514 nm (Ar), 532 nm (frequency doubled YAG).
Blue primary: 476 nm (Ar), 442 nm (HeCd).

The wavelength combination 633 - 532 - 442 nm was investigated in more detail since it resulted in the largest gamut from both theoretical and visual evaluation.

V. HOLOGRAM COMPUTATION

The algorithms used by our group are based on a simulation of the physical process of light interference[10]. The task of adapting these algorithms to multispectral images is relatively straightforward: one simply changes the wavelength of the simulated reference beam to the desired display wavelength. The angle of the reference beam is dictated by the geometry of the display. The optical properties or the TeO_2 crystal and the spatial frequencies of the beam registration HOE play an important role in the determination of this angle and will be discussed in the following sections.

VI. OPTICAL PROPERTIES OF THE AOM CRYSTAL

An adequate understanding of the optical behavior of the AOM material is essential in the course of this work. TeO_2 used in the shear mode is optically active[11]: right hand and left hand circularly polarized light propagating along the [001] direction have different indices of refraction, and plane polarized light has its plane of polarization rotated by:

$$\theta = \frac{2\pi n_o \delta}{\lambda} \qquad (1)$$

where n_o is the ordinary index of refraction and δ is the wavelength dependent index spliting between left and right-hand polarized light:

$$\delta = \frac{n_l - n_r}{2 n_o} \qquad (2)$$

An interesting property of the shear waves propagating in TeO_2 is that they will cause the direction of polarization of the diffracted light to be rotated by 90^o [11]. Thus, right-hand circularly polarized light will be diffracted into the left-handed mode, and vice-versa.

The practical implications of the optical activity of tellurium dioxide is that the isotropic Bragg relations usually encountered in optical holography are no longer applicable. One has to use instead the more complicated anisotropic Bragg relations developped by Dixon[12] and Warner et al[11] to determine the incident and diffracted beam angles. The authors refer to those two excellent papers for a thorough derivation of those relations. We will only describe here the relevant results.

The incident and diffracted internal angles θ_1 and θ_2 can be described by the equations:

$$\sin\theta_1 = \frac{\lambda}{2 n_o \Lambda} + \frac{2 n_o \Lambda \delta}{\lambda} + \frac{\sin^2\theta_1 \Lambda n_e^2 - n_o^2}{2\lambda}\left(\frac{n_e^2}{n_e^2}\right) \qquad (3a)$$

$$\sin\theta_2 = \frac{\lambda}{2 n_o \Lambda} - \frac{2 n_o \Lambda \delta}{\lambda} - \frac{\sin^2\theta_1 \Lambda n_e^2 - n_o^2}{2\lambda}\left(\frac{n_e^2}{n_e^2}\right) \qquad (3b)$$

where n_e is the extraordinary index of refraction and Λ is the wavelength of the shear waves in the crystal. Λ is related to the wave propagation speed v and the frequency of the electronic signal f by the formula:

$$\Lambda = \frac{v}{f} \qquad (4)$$

The first term in (3a) and (3b) represents ordinary Bragg reflection if there were no other effects. The additionnal terms are a consequence of the optical activity of TeO_2. The external angles to the crystal are derived from (3a) and (3b) by using snell's law:

$$\theta_{in} = n_o (1 + \delta)\, \theta_1 \qquad (5a)$$

$$\theta_{out} = n_o (1 - \delta)\, \theta_2 \qquad (5b)$$

where we have used the approximation $\sin(\theta) \approx \theta$ since all the relevant angles are small.

Figure 2. Experimental and calculated values of the θ_{in} as a function of acoustic frequency for several optical wavelengths (from ref. 11).

Figure 2 shows experimental and calculated values of the Bragg angle for various wavelengths. We see that the Bragg angle exhibits a broad minimum around a wavelength-dependent center frequency. The Bragg angle

thus varies very little over a wide spatial frequency range, as opposed to the usual isotropic case where the Bragg angle increases linearly for small angles. The practical consequence of this broad minimum is that it is possible to acheive good phase matching over a wide bandwidth with TeO_2, which results in very efficient devices operating over a wide frequency range[11].

VI. AOM GEOMETRY

Equations 3 to 5 give us a good starting point for the design of our color display. Our AOM has three identical channels exhibiting a bandpass of 50 MHz and a center frequency of 75 MHz. The incident angle of each wavelength on the crystal has to be carefully adjusted to permit an optimum AOM operation over the bandpass. A good starting point is to adjust the incident angle so that it coincides with the Bragg angle at each wavelength for the AOM center frequency. In practice, the incident angle is then fine-tuned by trial and error until the AOM response is flattest over the whole bandpass. This operation gives the following measured incident and diffracted wave angles for the wavelengths of interest to us:

wavelength	θ_{in} **(deg.)**	θ_{out} **(50 MHz)**	θ_{out} **(75 MHz)**	θ_{out} **(100 MHz)**
633 nm (red)	2.9	- 0.04	- 1.51	- 2.99
532 nm (green)	2.9	0.43	- 0.81	- 2.04
514 nm (green)	3.0	0.61	- 0.59	- 1.77
476 nm (blue)	3.3	1.09	- 0.02	- 1.12
442 nm (blue)	3.4	1.35	0.32	- 0.70

Table I. incident and diffracted angles on the AOM.

It is clear that the total diffracted range becomes smaller for the shorter wavelengths. As a result, the horizontal view zone is 30 percent smaller at 442 nm than at 633 nm. The diffracted angles at the center frequency also vary considerably with wavelength. Those center frequency angles, however, should be close to each other if we want the red, green, and blue components of the image to overlap correctly across the horizontal view zone.

The most obvious way to register the diffracted wavelength components is to redirect them into a common angular range by using prisms or gratings. We chose to implement second approach since the gratings could be fabricated in our laboratory.

6.2 HOE characteristics.

The first step in calculating the correct characteristics of our registration Holographic Optical Element (HOE) is to determine the best common angular range to which the beams should be rediffracted. Considering that both the AOM and the HOE have limited diffraction efficiencies leads to two "forbidden" angular ranges:

- The 2.9 to 3.4 degree range where the zeroth order of the AOM is present cannot be used.
- The -2.99 to 1.35 degree range is also forbidden because the zeroth order of the HOE is present.

Because the AOM is operated in the deep Bragg regime its extraneous diffracted orders have a very low intensity and can be neglected without image sacrifice in our calculations. This is not the case for the HOE, so

any solution will have to be inspected to be sure that higher HOE orders do not overlap on the image.

The grating will affect the image by a small amount of spherical aberration since the grating equation is not linear. This aberration will remain visually acceptable, however, if the spatial frequencies of the HOE are kept low enough since the grating equation is linear to within half a percent for angles smaller than 10 degrees.

The previous considerations led us to choose 5 degrees as the angle to which the center frequency should be rediffracted. The determination of the HOE spatial frequencies with the grating equation is then straightforward :

$$f = \frac{\sin(\theta_{out}) - \sin(\theta_{in})}{\lambda} \qquad (6)$$

where θ_{in} in Equation (6) is equivalent to θ_{out} (75 MHz) of Table I and θ_{out} of (6) equals five degrees. The results of this calculation are listed in Table II.

wavelength	**f (cycles / mm)**	**θ_{out} (50 MHz)**	**θ_{out} (75 MHz)**	**θ_{out} (100 MHz)**
633 nm (red)	179	6.47	5.0	3.51
532 nm (green)	190	6.23	5.0	3.75
514 nm (green)	190	6.22	5.0	3.83
476 nm (blue)	184	6.12	5.0	3.90
442 nm (blue)	185	6.05	5.0	3.99

Table II. Center frequency angle registration.

It is interesting to note that the gratings used for each wavelength differ at most by six percent from each other. This similarity inspired us to use a single grating having a spatial frequency of 185 cycles/mm as our HOE. With such a grating Table II then becomes:

wavelength	**f (cycles / mm)**	**θ_{out} (50 MHz)**	**θ_{out} (75 MHz)**	**θ_{out} (100 MHz)**
633 nm (red)	185	6.68	5.21	3.72
532 nm (green)	185	6.08	4.83	3.60
514 nm (green)	185	6.07	4.86	3.68
476 nm (blue)	185	6.15	5.03	3.93
442 nm (blue)	185	6.05	5.0	3.99

Table III. approximate center frequency angle registration with a single grating.

Although the center frequency angles are now slightly different, the final diffraction ranges still overlap and none of the narrow blue deflection range is lost. The action of the AOM - HOE combination of table 3 is depicted in Figure 3. The gap between the AOM and the HOE introduces a small horizontal translation between each color component. It is important to place the HOE as close as possible to the AOM as to minimize that effect. The residual horizontal translation can then be compensated for by software.

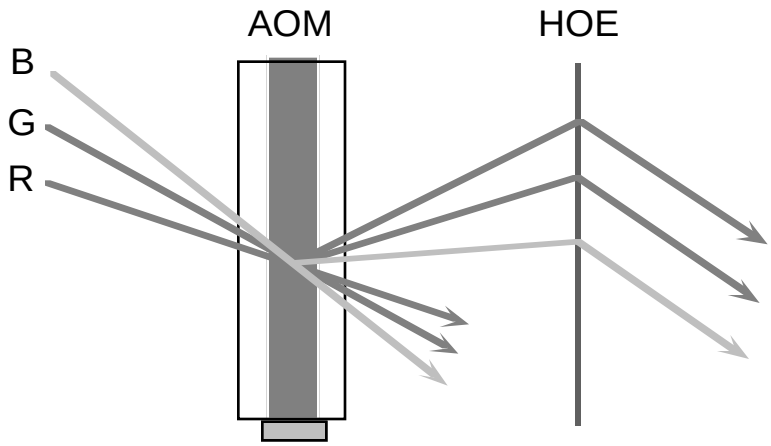

Figure 3. Angular registration with an HOE.

6.3 HOE manufacture

A number of HOE characteristics are desirable if we want a satisfactory display performance:

- The grating should be efficient over a wavelength range extending from the red to the blue components of the spectrum.
- Its angular selectivity should be very small over the angular range specified by Table 3.
- It should have very low scattering noise.

Meeting all these demands with a single grating is very difficult since they somewhat contradict each other. A good diffraction efficiency for small angles dictates the use of a thick medium, but chromatic and angular selectivity become significant for very thick media. The best overall results were obtained using 28 μm thick dichromated gelatin plates with a 110 mJ / cm^2 exposure at 514 nm. This resulted in a first order diffraction efficiency of 32 percent at 514 nm and an acceptable noise level. Diffraction efficiencies at 633 nm and 476 nm were about 25 percent.

VII. DISPLAY GEOMETRY

7.1 Horizontal geometry

The horizontal display geometry is shown on Figure 4 with the 633 - 532 - 442 nm combination. Each linearly polarized laser beam first passes through a quarter-wave plate which circularizes the polarization. The beams are then horizontally expanded to match the shape of the AOM's acoustic channels. Since the acoustic channels are 3mm wide there is no need for a vertical expansion of the laser beams. The red and green components have the same incident angle on the AOM and are expanded using a single cylindrical telescope. The acoustic channels are well separated vertically and mirrors are used to bring the three color primaries to

the correct incident angle. The beams are then diffracted by the AOM - HOE pair and are Fourier transformed by the achromat L_1 before being scanned by the polygonal mirror. The output lens L_3 is a 55 mm f/1.2 camera lens which exhibits very little chromatic aberration. The L_1 - L_3 lens combination multiplies the diffracted spatial frequencies by a factor of five, resulting in a horizontal view zone of 15 degrees at 633 nm, 12 degrees at 532 nm and 10 degrees at 442 nm.

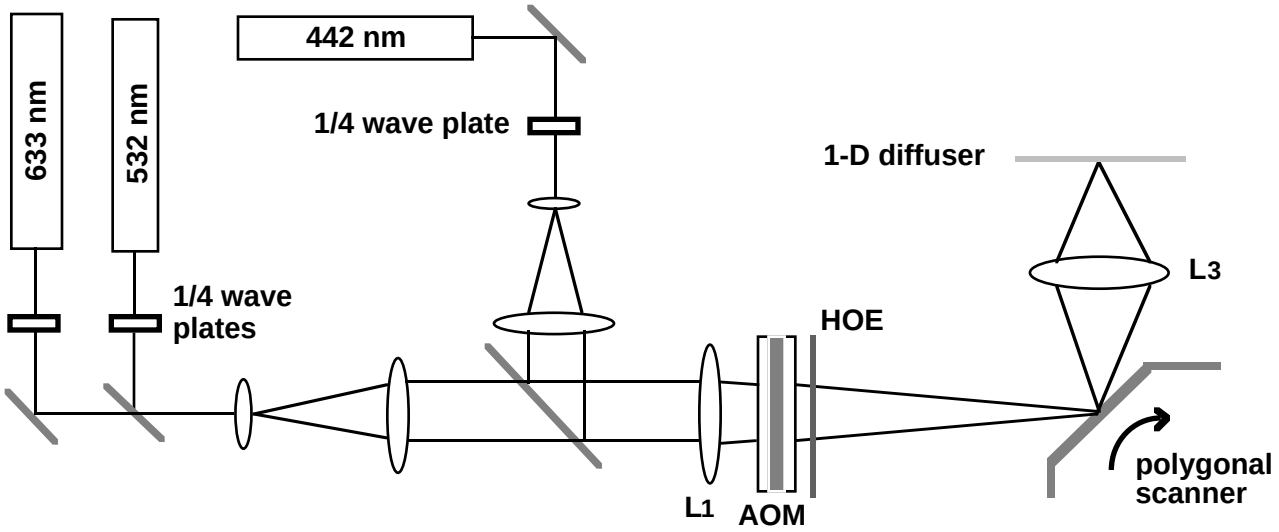

Figure 4. Display geometry (horizontal axis). The vertical scanning optics have been omitte

7.2 Vertical geometry

The vertical geometry is very similar to the one described previously[3] and is shown on Figure 5. Each AOM acoustic channel is 3.2 mm wide and the center to center channel separation is 4.7 mm. The interchannel crosstalk is less than -30 db across the channel length and thus it is visually unnoticeable[3]. The optical system of Fig. 5 registers the three primary colors at the same vertical focus, with the result that the red, green and blue scan lines are superimposed instead of being displayed side by side as in normal television. The last element in the optical system is an on-axis vertical diffuser which provides a comfortable vertical view zone while leaving the horizontal component of the image unaltered. The diffuser was designed and fabricated by Michael Klug of the Media Laboratory. More details about this important holographic optical element can be found in ref. 13.

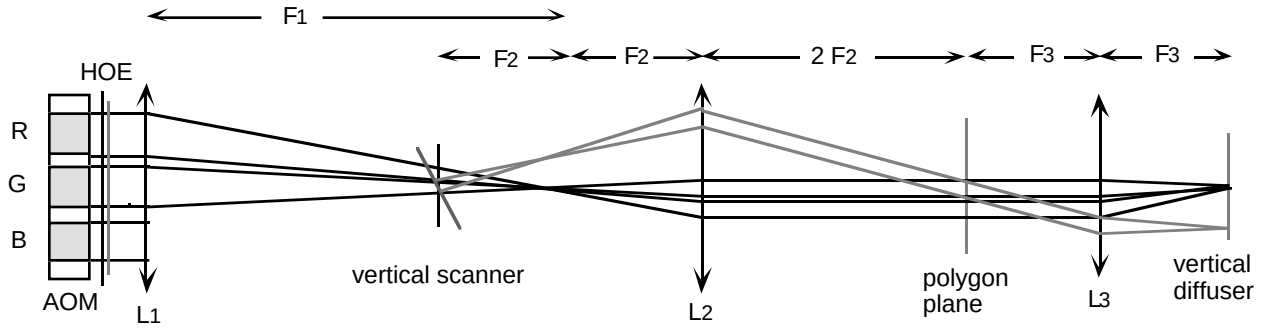

Figure 5. Vertical display geometry

VIII. RESULTS

8.1 Visual evaluation

The display performance proves to be visually very acceptable, as demonstrated by figures 6a and 6b. The displayed images are crisp and exhibit good contrast. The color registration is excellent thourough the view zone, except for the first and last few scan lines where a slight vertical misregistration is noticeable. Virtually all this misregistration can be attributed to the cylindrical lens doublet L_2 of Fig.5 which is not corrected for chromatic aberration. Using a cylindrical achromatic doublet would easily solve this problem but such an element would have to be custom manufactured. There is a slight color shift across the image. Two factors principally contribute to this effect: The AOM frequency response is not flat across the RF spectrum, and the DCG grating exhibits a small angular selectivity. This color shift, however, is rather difficult to notice without measuring instruments.

Figure 6. Two computer generated images displayed by the system. (a) set of Munsell chips. (b) a single frame of an animated sequence. A full color version of (6a) and (6b is printed on page of the proceedings.

A faint background noise is noticeable across the image. Scattering from the registration HOE proves to be the principal source of this noise, whose overall effect is to reduce the effective gamut of the display. The gamut still remains larger than can be obtained by CRT monitors. There is no doubt, however, that the image quality would greatly benefit from lower noise HOE.

As explained in section VI, the blue and green image components drop off at the extreme edges of the horizontal view zone. There is no simple way to compensate for this effect, since it stems from the physics of the diffraction process.

8.2 Color measurements

Measurements made on the holovideo system can be plotted on the 1976 CIE chromaticity diagram that is commonly used for color analysis. The dashed triangle in figure 7a connects the red, green, and blue primaries measured on the system. This triangle encompasses all possible points obtainable by the holographic video display. By subtracting components measured from a black image (that consists purely of the noise mentioned in section 8.1) the gamut would increase to the larger triangle that touches the spectral locus. Although noise does shrink the gamut measured on the MIT color holovideo display, the gamut is still greater than that obtained from a conventional (2-dimensional) high resolution CRT color monitor (shown by dotted lines).

In figure 7b several color points are plotted. The yellow point and the less saturated red and green points were

measured from the donuts hologram shown in figure 6b. The blue and purple images were measured from the Munsell chips hologram of fig. 6a. The system was color balanced to a reference white (shown by a + in figure 7b) that is similar to CIE illuminant D65 (this white was obtained from a standard slide projector source). The reference white point can easily be changed by varying the laser powers and measuring the output. It is interesting to note that our reference white point would seem yellowish when compared to the blue biased monitor.

By using this combination of laser wavelengths we obtain a large gamut of color that encompasses most colors that we can perceive. Even when noise is added to the system, the gamut is large enough to produce almost all colors found in nature. The quality of color obtained from this combination of laser wavelengths was superior to that found using other wavelength combinations. In particular, the use of the 514 nm Argon laser line gave unsatisfactory yellow image compared to that obtained using the 532 nm Nd:YAG line.

Figure 7. (a) The 1976 CIE chromaticity diagram shows how the color gamut of the MIT
system (dashed line) is substantially larger than the gamut obtained from a high-re
dimensional color monitor (dotted line). The gamut size increases to the border of the s
when noise is removed from the system (solid line). (b) Measured color points from t
shown in figures 6a and 6b.

IX. CONCLUSION

We have demonstrated the possibility of displaying good quality animated color holograms with our scanned acousto-optic deflector approach. The images exhibit a large color gamut and excellent color registration. The signal to noise ratio is acceptable but leaves room for improvement. Better results could probably be obtained by using three different gratings tailored to each individual wavelength instead of the single element described in this paper.

We are now working on the implementation of a much larger system which should eventually be capable of displaying 36 million samples per frame at a refresh rate of 40 frames / second. Much work remains to be done before before electronic holography displays become a practical tool, but we are convinced that our efforts and those of others will eventually lead to useful devices.

X. ACKNOWLEDGMENTS

The authors would like to thank Michael H. Klug who developped the vertical diffuser HOE and Wendy J. Plesniak who contributed to some of the computer images. We also thank A.B. Lasers for lending us the frequency-doubled ND:YAG laser used in our experiments.

The research described here has been sponsored by the Defense Advanced Research Projects Agency through the Rome Air Development Center (contract F30602-89-C0022), and the Television of Tomorrow research consortium of the MIT Media Laboratory.

XI. REFERENCES

1. P. St Hilaire, S.A. Benton *et al.* ,"Electronic Display System for Computational Holography", *SPIE Proceedings*, Vol. #1212 "Practical Holography IV", 1990, S.A. Benton, editor.

2. P. St Hilaire, S.A. Benton, "Synthetic Aperture Holography: A New Approach to Three Dimensional Displays", Submitted to *Journal of the Optical Society of America A*, Oct. 1991.

3. S.A. Benton, "Experiments in holographic video" , *SPIE Proceedings* , Vol. #IS-8 , paper #IS8-05.

4. P. St-Hilaire, S.A. Benton *et al.*, "Real-time holographic display: Improvements using a multichannel acousto-optic modulator and holographic optical elements", *SPIE Proceedings*, Vol. #1461 "Practical Holography V", 1991, S.A. Benton, editor.

5. L. Bademian, "Parallel-Channel Acousto-Optic Modulation", *Optical Engineering*, vol. 25, pp 303-308, Feb 1986.

6. T. Kubota, "Recording of High Quality Color Holograms", *Appl. Opt.* 25, 4141 -4145 (1986).

7. J. L. Walker and S.A. Benton, "In Situ Swelling for Holographic Color Control.", *SPIE Proceedings*, Vol. 1051 "Practical Holography III", (1989), S.A. Benton editor.

8. P. Hubel and L. Solymar, "Color-Reflection Holography: Theory and Experiment", *Appl. Opt.*, vol. 30, No. 29, pp 4190-4203 (0ct. 1991).

9. P.M. Hubel, "Recent Advances in Color Reflection Holography", *SPIE Proceedings* , Vol. 1461 "Practical Holography V", (1991), S.A. Benton editor.

10. M. Lucente, "Optimization of Hologram Computation for real-time display", *SPIE. Proceedings*, Vol. 1667 "Practical Holography VI" (1992), *To be published.*

11. A.W. Warner, D.L. White, W.A. Bonner, "Acousto-optic Light Deflectors Using Optical Activity in Paratellurite", *J. Appl. Phys.*, Vol. 43, No 11, Nov. 1972.

12. R.W. Dixon, *IEEE J. Quantum Electron.* , 3 , 85 (1967).

13. M.A. Klug, "Holographic Optical Elements for Holographic Stereogram Printers", S.M. Thesis, Massachussetts Institute of Technology, June 1991.